Genome Scans for Transmission Ratio Distortion Regions in Mice

Joaquim Casellas,*,†,1 Rodrigo J. Gularte,†,1 Charles R. Farber,†,‡ Luis Varona,§ Margarete Mehrabian, Eric E. Schadt,†† Aldon J. Lusis,** Alan D. Attie,‡‡ Brian S. Yandell,§§ and Juan F. Medrano†,2**

*Departament de Ciència Animal i dels Aliments, Universitat Autònoma de Barcelona, 08193 Bellaterra, Spain, †Department of Animal Science, University of California, Davis, California 95616-8521, ‡Departments of Medicine, Biochemistry and Molecular Genetics and Center for Public Health Genomics, University of Virginia, Charlottesville, Virginia 22908, §Departamento de Anatomía, Embriología y Genética Animal, Universidad de Zaragoza, 50013 Zaragoza, Spain, **Department of Medicine, David Geffen School of Medicine, University of California, Los Angeles, California 90095-1679, ††Rosetta Inpharmatics, Seattle, Washington 98109, ‡‡Department of Biochemistry and §§Departments of Statistics and Horticulture, University of Wisconsin, Madison, Wisconsin 53706

ABSTRACT Transmission ratio distortion (TRD) is the departure from the expected genotypic frequencies under Mendelian inheritance. This departure can be due to multiple physiological mechanisms during gametogenesis, fertilization, fetal and embryonic development, and early neonatal life. Although a few TRD *loci* have been reported in mouse, inheritance patterns have never been evaluated for TRD. In this article, we developed a Bayesian binomial model accounting for additive and dominant deviation TRD mechanisms. Moreover, this model was used to perform genome-wide scans for TRD quantitative trait loci (QTL) on six F_2 mouse crosses involving between 296 and 541 mice and between 72 and 1854 genetic markers. Statistical significance of each model was checked at each genetic marker with Bayes factors. Genome scans revealed overdominance TRD QTL located in mouse chromosomes 1, 2, 12, 13, and 14 and additive TRD QTL in mouse chromosomes 2, 3, and 15, although these results did not replicate across mouse crosses. This research contributes new statistical tools for the analysis of specific genetic patterns involved in TRD in F_2 populations, our results suggesting a relevant incidence of TRD phenomena in mouse with important implications for both statistical analyses and biological research.

TRANSMISSION ratio distortion (TRD) is defined as a significant departure from the expected Mendelian inheritance ratio of genetic *loci* in offspring (Silver 1993; Crow 1999; Merill *et al.* 1999; Pardo-Manuel de Villena *et al.* 2000a). This phenomenon has been reported in a broad range of organisms including mammals (Canham *et al.* 1970; Evans *et al.* 1994; Vorechovsky *et al.* 1999), insects (Nur 1977), and plants (Rhoades 1942; Vongs *et al.* 1993). Several biological mechanisms can cause TRD, including the preferential transmission of one of the two alleles carried by a heterozygote to the zygote at the time of fertilization (Agulnik *et al.* 1990; Lyon 1991; Dyer *et al.* 2007), also known as meiotic drive, as well as embryo or fetal failure (Wakasugi 1974) or differential viability during early neonatal life under a given genotype (Moore 2006). In mouse, the most studied example of TRD involves the *t* complex on chromosome 17 for which homozygous males are sterile and heterozygous males transmit the *t* haplotype to >50% of their progeny (Silver 1985; Lyon 1991). Although the effect of the *t* haplotype in TRD is known, little is known about the presence of additional genomic regions involved in TRD on other mouse chromosomes.

Previous studies of TRD were focused on backcross populations (Montagutelli *et al.* 1996; Shendure *et al.* 1998; de la Casa-Esperón *et al.* 2000; Pardo-Manuel de Villena *et al.* 2000a; Vogl and Xu 2000), where only departures from the expected 50% heterozygous–50% homozygous ratio could be assessed. This experimental design allowed for a straightforward analysis of the segregation departure, often with a standard χ^2- (Paz-Miguel *et al.* 2001; Underkoffler *et al.* 2005) or *t*-test (Shendure *et al.* 1998), although this masked the genetic mechanism (or inheritance model) involved in the departure. The previously reported departures from the homozygous–heterozygous

doi: 10.1534/genetics.111.135988
Manuscript received October 20, 2011; accepted for publication January 22, 2012
[1]These authors contributed equally to this work.
[2]Corresponding author: Department of Animal Science, University of California, One Shields Ave., Davis, CA 95616-8512. E-mail: jfmedrano@ucdavis.edu

ratio in backcrosses characterized the joint contribution of the additive and dominant genetic effects, without discriminating between both sources of genetic variation. Hence, the inheritance model of TRD remains unexplained. According to Falconer and Mackay (1996), F_2 populations are a preferable cross design to assess both additive and dominant effects for a given *locus*, although there are not adequate models to account for these genetic contributions to TRD.

From a Bayesian point of view, comparison between alternative models is developed by calculating Bayes factors (BFs) (Kass and Raftery 1995), the ratio between the marginal probabilities of the data given the tested models. Bayes factors do not depend upon asymptotic properties of frequentist estimators and avoid the calculation of significance levels (Stram and Lee 1994). In addition, BFs behave well, even when the bounded variable to be tested is close to the boundary of the parametric space (García-Cortés *et al.* 2001), this being common in TRD when a given genotype completely disappears in the F_2 population (Merkle *et al.* 1992). The Verdinelli and Wasserman (1995) BF has been recently adapted to test additive and dominant quantitative trait loci (QTL) on phenotypic traits (Casellas *et al.* 2008b) and was suggested as a very appealing tool to examine statistical relevance of additive and/or dominant sources of variation linked with genomic markers.

This article focuses on two major objectives. First, Verdinelli and Wasserman's (1995) BF was adapted to map TRD QTL in F_2 populations under different inheritance models. The analytical approaches were implemented in Fortran90 programs and they are available upon request from the first author of this article (J. Casellas). Second, genome scans for TRD QTL were performed on six F_2 mouse crosses to characterize the distribution and genetic model of TRD in the mouse genome.

Materials and Methods

Transmission ratio distortion analysis

Analytical model: Take a data set with n individuals genotyped by an autosomal *locus* with alleles A_1 and A_2, where $n_{A_1A_1}$, $n_{A_1A_2}$, and $n_{A_2A_2}$ are the numbers of individuals with genotypes A_1A_1, A_1A_2, and A_2A_2, respectively ($n = n_{A_1A_1} + n_{A_1A_2} + n_{A_2A_2}$). Under a flexible inheritance model, the probability of each genotype to be sampled in the F_2 population can be written as

$$p(A_1A_1|\mathrm{F}_2) = \frac{1}{4}\frac{(1-|2a|\kappa_\mathrm{a}-|d|\kappa_\mathrm{d})}{(1-|a|-|d|/2)}$$

$$p(A_1A_2|\mathrm{F}_2) = \frac{1}{2}\frac{[1-|a|-|d|(1-\kappa_\mathrm{d})]}{(1-|a|-|d|/2)}$$

$$p(A_2A_2|\mathrm{F}_2) = \frac{1}{4}\frac{[1-|2a|(1-\kappa_\mathrm{a})-|d|\kappa_\mathrm{d}]}{(1-|a|-|d|/2)},$$

where a and d are appropriate parameters modeling additive and dominance (or overdominance) phenomena on TRD, respectively, κ_a is an indicator variable equal to 1 if $a \geq 0$ and 0 otherwise, and κ_d is an indicator variable equal to 1 if $d \geq 0$ and 0 otherwise. More specifically, a accounts for the additive allelic substitution effect compromising the viability of some genotypes and d accounts for the dominance (or overdominance) deviation defined as the fitness departure of the heterozygote over the average fitness of the two homozygotes (Falconer and Mackay 1996). Taking the probability of an A_1A_1 genotype as an example, the first element in the above expression accounts for the expected genotypic frequency from an F_2 segregation without transmission distortions ($\frac{1}{4}$), and the second element accounts for the probability of the A_1A_1 genotype to be sampled in the F_2 population ($1-|2a|\kappa_\mathrm{a}-|d|\kappa_\mathrm{d}$; numerator) and corrected for the overall losses of individuals in terms of genotypic frequency ($\frac{1}{4}(1-|2a|-|d|)+\frac{1}{2}(1-|a|)+\frac{1}{4}(1-|d|)=\frac{1}{4}(1-|2a|)+\frac{1}{2}(1-|a|-|d|)+\frac{1}{4}=1-|a|-|d|/2$; denominator). This correction factor guarantees $p(A_1A_1|\mathrm{F}_2)+p(A_1A_2|\mathrm{F}_2)+p(A_2A_2|\mathrm{F}_2)=1$. See examples in Table 1 for a collection of genotypic frequencies and transmission ratio distortion effects.

Table 1 Examples of genotypic frequencies resulting from different combinations of values for additive (*a*), dominance (*d*), and overdominance (*h*) parameters of the transmission ratio distortion model

Genotypic frequencies			TRD effects	
A_1A_1	A_1A_2 or A_2A_1	A_2A_2	*a*	*d*
1/4	1/2	1/4	0	0
1	0	0	−1/2	−1/2
0	1	0	0	1
0	0	1	1/2	−1/2
1/2	1/2	0	−1/2	0
1/2	0	1/2	0	−1
0	1/2	1/2	1/2	0
1/3	1/3	1/3	0	−1/2

Bayesian implementation of the TRD model: The conditional posterior probability of the TRD parameters can be described within a Bayesian context as $p(a,d \mid \mathbf{y}) \propto p(\mathbf{y} \mid a,d)\, p(d \mid a)\, p(a)$, where $\mathbf{y}$ is the column vector of genotypes. The conditional probability of a given genotype [*e.g.*, $p(A_1A_1|\mathrm{F}_2)$] can be viewed as the success probability of a Bernoulli variable with failure probability $1-p(A_1A_1|\mathrm{F}_2)$ (*i.e.*, genotypes A_1A_2 and A_2A_2). In the likelihood, the genotype of all the individuals for a given SNP becomes a multinomial distribution as follows:

$$p(a,\, d|\, y) = \frac{n!}{n_{A_1A_1}!n_{A_1A_2}!n_{A_2A_2}!}[p(A_1A_1|\mathrm{F}_2)]^{n_{A_1A_1}} \times [p(A_1A_2|\mathrm{F}_2)]^{n_{A_1A_2}}[p(A_2A_2|\ \mathrm{F}_2)]^{n_{A_2A_2}}.$$

Given the lack of previous knowledge about the inheritance model of transmission distortions and the magnitude of their effects, a flat prior between appropriate bounds (see below) can be assumed for a and d.

Bayes factor analysis for checking a and d relevance: The BF is the standard Bayesian tool to compare models and

focuses on the ratio between the posterior probability of the two competing models (Kass and Raftery 1995). A BF > 1 supports the numerator model whereas a BF < 1 favors the denominator model. The Verdinelli and Wasserman (1995) BF compares two nested models that differ in one or a few bounded variables and requires the analysis of only the most complex model (García-Cortés *et al.* 2001; Varona *et al.* 2001). The key step for this calculation is the definition of appropriate proper priors for the parameters of interest. In our case, prior distribution for a was assumed to be

$$p(a) = 1 \quad \text{if} \quad a \in \left[-\frac{1}{2},\ \frac{1}{2}\right] \text{ and 0 otherwise,}$$

where 0 implied null transmission distortion and $\frac{1}{2}$ (or $-\frac{1}{2}$) characterized the extreme situation where all deleterious homozygotes and half of the heterozygotes disappear. On the other hand, the prior distribution for d was stated as

$$p(d \mid a) = \frac{1}{2-3|a|} \quad \text{if} \quad d \in [|a|-1,\ 1-2|a|] \text{ and 0 otherwise,}$$

where null transmission distortion ($d = 0$), loss of all heterozygotes ($d = |a|-1$), and loss of all possible homozygotes in the F_2 population ($d = 1-2|a|$) were characterized by appropriate values. Following Varona *et al.* (2001) and assuming parameter a as an example, the BF_a of the model including a and d against a virtual model with parameter d tests for the statistical relevance of a and can be straightforwardly calculated as

$$BF_a = \frac{p(a=0)}{p(a=0 \mid \mathbf{y})}.$$

Note that $p(a = 0)$ was previously defined by the prior probability of a [*i.e.*, $p(a = 0) = 1$], and therefore, $p(a = 0 \mid \mathbf{y})$ sufficed to obtain the BF. The same approach can be used to compute BF_d by assuming $p(d = 0) = 1/(2-3|a|)$. For each Monte Carlo Markov chain (MCMC) iteration, $p(a = 0 \mid \mathbf{y})$ and $p(d = 0 \mid \mathbf{y})$ can be calculated on the basis of the marginal posterior distribution of a and d, respectively, by applying the Rao–Blackwell kernel density estimation (Gelfand and Smith 1990; Wang *et al.* 1994).

Examples from simulated data

The performance of the TRD BF was outlined by simulation. Three different scenarios were characterized (null TRD, additive TRD, and dominance TRD), each one of them including 1000 replicates. Whereas population size was fixed to 250 individuals for additive and dominance TRD scenarios, this ranged between 100 and 500 individuals for the null TRD scenario. Stochastic simulations focused on a biallelic genetic marker where genotypic frequencies were defined by $p(A_1A_1 \mid F_2)$, $p(A_1A_1 \mid F_2)$, and $p(A_1A_1 \mid F_2)$ as stated above. The only genetic differences across scenarios were the values assumed for parameters a and d. The null TRD scenario fixed $a = 0$ and $d = 0$, whereas the additive TRD scenario kept $d = 0$ although sampled a population-specific random value between 0 and 0.5 for a. In a similar way, the dominance TRD scenario assumed $a = 0$ and picked a population-specific random value between -1 and 1 for d. Each population was analyzed by the Bayesian binomial model developed in this article and the BF was calculated for both TRD parameters. Conditional probabilities $p(a = 0 \mid \mathbf{y})$ and $p(d = 0 \mid \mathbf{y})$ were calculated for each MCMC iteration by using Rao–Blackwell kernel density estimation (Gelfand and Smith 1990; Wang *et al.* 1994) with a bin width of 0.005. A unique sampling chain of 100,000 iterations was launched for each analysis, discarding the first 10,000 iterations as burn-in. To compare this BF with standard statistical approaches, departures from the expected 0.25:0.5:0.25 genotypic frequencies were tested in all data sets by applying a χ^2-test with 2 d.f.

Examples from F_2 mouse genotypic data

The TRD model was applied in six F_2 mouse populations. All procedures of housing and treatment of animals were performed in accordance with Institutional Animal Care and Use Committee regulations and the American Association for Accreditation of Laboratory Animal Care (http://www.aaalac.org).

C57BL/6J × CAST/EiJ (cross 1): As previously described by Schadt *et al.* (2008), F_1 mice from C57BL/6J (B6) and CAST/EiJ (CAST) inbred strains were intercrossed to generate 296 F_2 progeny. F_2 mice were killed at 18 wk of age and kidneys were dissected and flash frozen in liquid nitrogen. Genomic DNA was isolated from kidneys by phenol-chloroform extraction. Genotyping was conducted by ParAllele BioScience (South San Francisco, CA), using the molecular-inversion probe multiplex technique (Hardenbol *et al.* 2005). Single-nucleotide polymorphisms (SNPs) were annotated using the NCBI Build 37.1 genome assembly. Full genotyping data on 1375 polymorphic SNPs were available for the 296 F_2 mice.

C57BL/6J$^{hg/hg}$ × CAST/EiJ (cross 2): This F_2 population was produced by crossing a *C57BL/6J$^{hg/hg}$* ($B6^{hg/hg}$) male with several CAST females, originating 75 F_1 individuals and 1132 F_2 individuals (Corva *et al.* 2001). Note that the $B6^{hg/hg}$ strain was isogenic to B6, except for the high-growth (*hg*) mutation on mouse chromosome 10 (Horvat and Medrano 2001; Wong *et al.* 2002) and a stretch of AKR/J sequence around this mutation (Horvat and Medrano 1996). This cross originated 596 F_2 heterozygote mice for the *hg* mutation (+/hg), 262 with genotype *hg/hg* and 274 with genotype +/+. Only *hg/hg* and +/+ F_2 mice were genotyped for 72 and 40 polymorphic microsatellite markers, respectively, distributed in all the autosomal chromosomes. Genotypic data per SNP were available for >98% of the F_2 individuals. Note that genetic markers in chromosome 10 were discarded for TRD analyses due to the arbitrary selection of mice according to their *hg* genotype. These mice were killed 9 wk after birth

and a spleen sample was stored and frozen. Genotyping was performed from spleen DNA according to conventional PCR and agarose gel electrophoresis methods (Corva *et al.* 2001).

C57BL/6J × C3H/HeJ (cross 3): The F_2 cross between B6 and C3H/HeJ (C3H) mice originated 321 F_2 progeny, and 309 individuals were available for genotyping for 1147 autosomal SNP markers. Mice were slaughtered at 20 wk of age and livers were collected and flash frozen in liquid nitrogen. DNA extraction and genotyping followed the procedures described for cross 1. Only those SNP markers with genotypic information for >95% of the individuals were kept for the analysis of TRD QTL.

B6.apoE$^{-/-}$ × C3H.apoE$^{-/-}$ (cross 4): As described by Shi *et al.* (2000), founder B6 apoE null (B6.apoE$^{-/-}$) mice were purchased from the Jackson Laboratory (Bar Harbor, ME). The C3H/HeJ apoE null (C3H.apoE$^{-/-}$) mice were bred by backcrossing B6.apoE$^{-/-}$ to C3H for 10 generations. F_1 mice were generated by constructing reciprocal crosses between B6.apoE$^{-/-}$ and C3H.apoE$^{-/-}$, and F_2 mice were subsequently bred by intercrossing the F_1 mice. These mice were killed at an age of 24 wk and livers were collected and flash frozen in liquid nitrogen. Genotyping followed the procedures described for cross 1. A total of 332 F_2 mice were available (Schadt *et al.* 2008) and 322 of them were genotyped for a custom panel of SNP markers. After excluding those SNPs with data for <95% of the genotyped mice, 1182 SNPs located in all the autosomal chromosomes were used for the analyses.

C57BL/6$^{ob/ob}$ × BTBR$^{ob/ob}$ (crosses 5 and 6): BTBR and C57BL/6J$^{ob/+}$ (B6$^{ob/+}$) were purchased from The Jackson Laboratory and kept in the vivarium of the University of Wisconsin (Madison, WI). Note that B6$^{ob/+}$ mice were heterozygous for the *ob* mutation in the Leptin gene located on mouse chromosome 6 (Ingalls *et al.* 1950; Zhang *et al.* 1994). The experimental design for both crosses 5 and 6 started with the mating of BTBR$^{ob/ob}$ and B6$^{ob/ob}$ mice to generate $F_1{}^{ob/ob}$ individuals. The $F_1{}^{ob/ob}$ individuals were intercrossed and $F_2{}^{ob/ob}$ individuals were used for genotyping purposes. DNA was extracted from tail-clip samples by conventional methods for 477 (cross 5) and 541 (cross 6) $F_2{}^{ob/ob}$ mice. The mice from cross 5 were genotyped for 192 microsatellite markers distributed along the autosomal chromosomes with the exception of mouse chromosome 6. Note that the *ob* mutation was located in this chromosome and the preselection of $F_2{}^{ob/ob}$ mice invalidates any further result about TRD in this chromosome. On the other hand, cross 6 was genotyped with a custom panel of 1854 SNP markers located in all autosomal chromosomes except chromosome 6. Percentages of missing genotypes were <69% and 9% in cross 5 and cross 6, respectively.

Markov chain Monte Carlo analyses: Marker-by-marker genotypic frequencies were analyzed under the TRD model developed above. Metropolis–Hastings sampling (Hastings 1970) was used to obtain autocorrelated samples of a and d from their marginal posterior distribution. A unique chain of 100,000 elements was launched for each genetic marker and inheritance model, after discarding the first 10,000 elements as burn-in. Convergence was checked by visual inspection and by the Raftery and Lewis (1992) approach, providing burn-in periods (<50) smaller than the number of discarded elements. All correlated samples were used to calculate the posterior mean and standard deviation of a and d.

Correction for multiple testing: Taking BF_a as an example, the posterior odds (PO) between the two competing models can be calculated as $PO_a = BF_a \times p_a \,/\, p_0$ (Kass and Raftery 1995), where p_a is the prior probability of the model including a, and p_0 is the prior probability of the model with $a = 0$. PO_a can be viewed as a weighted BF accounting for more realistic prior probabilities for both models under multiple testing. The prior probabilities of both models could be appropriately defined depending on our degree of belief on the expected number of markers showing transmission ratio distortion. In the standard development of the BF described above, we assumed that the ratio between p_a and p_0 (prior odds) was 1 and the prior probabilities for both competing models were 0.5 and 0.5 at each genetic marker, providing a huge *a priori* expected number of markers with transmission distortion. Given that the decline in linkage disequilibrium (LD) is an exponential function of distance, LD being very small for distances >20–30 cM (Sargolzaei *et al.* 2008), we divided the 19 autosomal chromosomes into 52 regions spanning 30 cM each that we assumed to be independent. Following Vidal *et al.* (2005) and Casellas *et al.* (2008), and under a conservative *a priori* criterion assuming a unique chromosomal region with transmission ratio distortion, the prior probabilities of the model including a and the model with $a = 0$ became $\frac{1}{52}$ and $\frac{51}{52}$ at each marker, respectively. Thus, PO_a can be easily obtained as $PO_a = BF_a \times \frac{1}{51}$. The same correction was applied to BF_d.

Alternatively, the distribution of the BF under null TRD effects was evaluated by 10,000 permutations at each TRD QTL peak. Each permutation involved (1) the simulation of a new data set with the same number of genotypes as in the original data set and with genotype probabilities 0.25 (A_1A_1), 0.5 (A_1A_2), and 0.25 (A_2A_2) and (2) the analysis of this synthetic data set under the TRD model. Posterior odds were obtained by the approach detailed above and the upper bound for the BF under the null hypothesis was assumed as the value in the 95th percentile.

Frequentist analysis: To check the statistical performance of the BF, departures from the expected genotypic frequencies in the F_2 populations were checked marker-by-marker by a standard χ^2-test with 2 d.f. For each population a standard Bonferroni correction (Bonferroni 1930) was applied to account for multiple testing under *a priori* $\alpha = 0.05$.

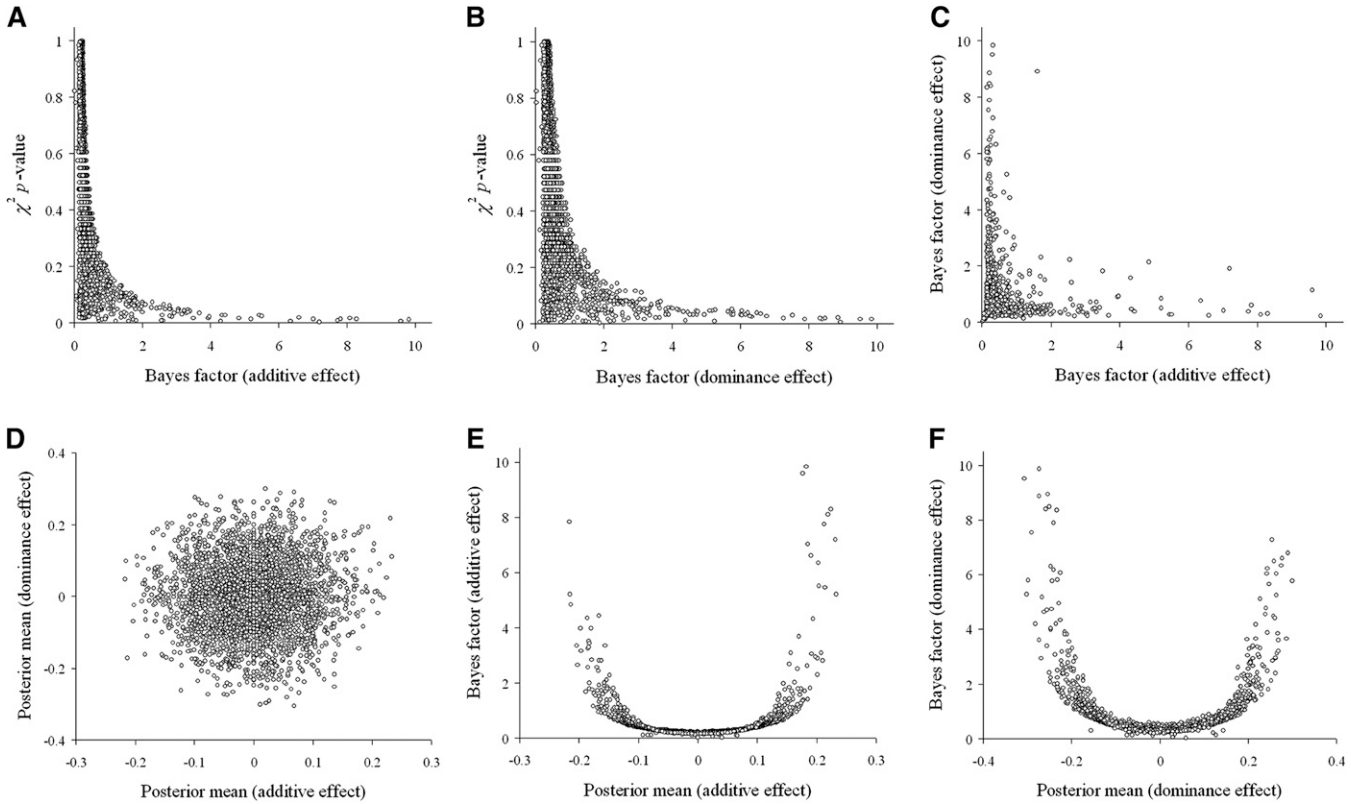

Figure 1 Performance of the Bayes factor (BF) for testing additive and dominance transmission ratio distortions (TRD) under null TRD departures. Stochastic simulation processes were used to generate 1000 populations with variable size ranging between 100 and 500 individuals. Genetic data were restricted to a single biallelic marker (alleles A_1 and A_2)with genotypic frequencies of 0.25 (A_1A_1), 0.5 (A_1A_2), and 0.25 (A_2A_2). For each population, genetic data were analyzed under the BF approach developed above and by launching a unique Monte Carlo Markov chain of 100,000 elements; the first 10,000 iterations were discarded as burn-in. Moreover, TRD was also tested by applying a standard χ^2-test with 2 d.f. Pairwise relationships are plotted, involving four parameters from the Bayesian analysis, *i.e.*, BFs for additive (elements A, C, and E) and dominance (elements B, C, and F) TRD and posterior means of the additive (elements D and E) and dominance (elements D and F) effects, as well as the *P*-value (elements A and B) derived from the frequentist χ^2-test.

Results

Analyses of simulated genotypic data

When genotypic frequencies were set to 0.25:0.5:0.25 (null TRD), the BF analysis discarded additive TRD in 95.6% of the simulations (Figure 1A), whereas this percentage reduced to 94.7% for dominance TRD (Figure 1B). In a similar way, χ^2-tests provided similar performances with 95.2% of the *P*-values being >0.05 (Figure 1, A and B). It is important to highlight that maximum BF estimates under the null TRD scenario were <10 in all cases. Figure 1, C and D, ruled out any kind of statistical relationship between the BF for additive TRD and the BF for dominance TRD, as well as for the estimated additive and dominance effects. Nevertheless, BFs for additive (dominance) TRD provided a U-shaped distribution when plotted against estimated additive (dominance) TRD effects (Figure 1, E and F); this distribution was centered on zero, there being located the minimum BF estimates.

A total of 71.3% of the BFs for additive TRD under the additive TRD scenario revealed statistical evidence for this biological phenomenon, this percentage being close to the 69.3% of the <0.05 χ^2 *P*-values. As evidenced by the almost linear trend shown in Figure 2A, both statistics performed similarly and revealed departures from the expected 0.25:0.5:0.25 in a comparable way. When plotted against the posterior mean for the additive TRD effect, the BFs also suggested a U-shaped distribution, this accumulating smallest BF values around zero, although overexpressing the right-hand side of the distribution with increasing BFs (Figure 2F). Indeed, a direct and strict relationship between the estimated additive TRD effect and its corresponding BF was without doubt, as well as the direct and linear relationship between the estimated and simulated additive TRD effect (Figure 2E). Dominance TRD effects were discarded in 92.1% of the analyses (Figure 2B), and any linear relationship between additive and dominance TRD parameters was discarded in Figure 2, C and D. Although not shown, dominance TRD simulations provided similar performances to those of the additive scenario.

Genome scan and model comparison

Under a standard frequentist approach (χ^2-test with 2 d.f.), significant departures from the expected genotypic frequencies in F_2 populations were not observed in mouse crosses 1,

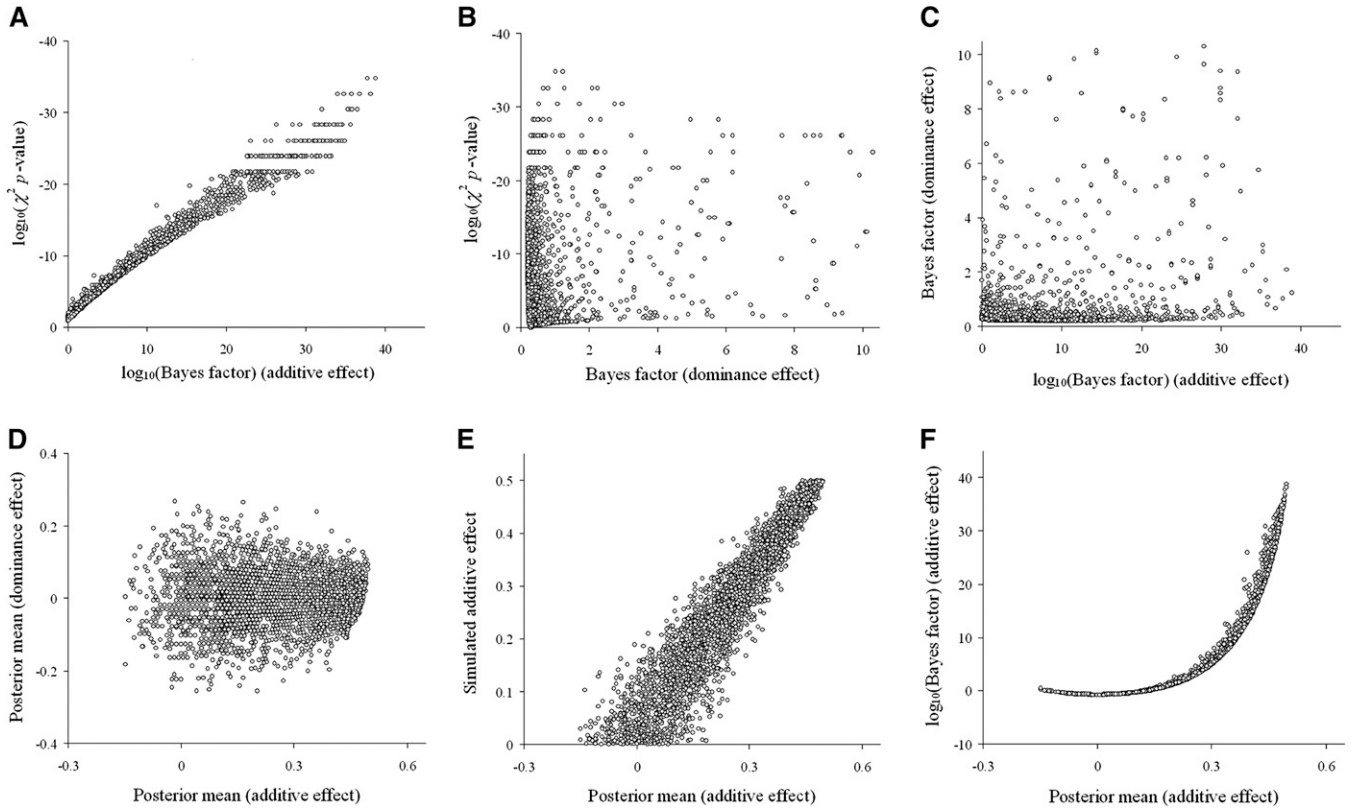

Figure 2 Performance of the Bayes factor (BF) for testing additive and dominance transmission ratio distortions (TRD) under additive TRD departures. Stochastic simulation processes were used to generate 1000 populations with 250 individuals each. Genetic data restricted to a single biallelic marker (alleles A_1 and A_2) and genotypic frequencies were generated under an additive TRD effect ranging from 0 to 0.5. For each population, genetic data were analyzed under the BF approach and by launching a unique Monte Carlo Markov chain of 100,000 elements; the first 10,000 iterations were discarded as burn-in. Moreover, TRD was also tested by applying a standard χ^2-test with 2 d.f. Pairwise relationships are plotted, involving four parameters from the Bayesian analysis, *i.e.*, BFs for additive (elements A, C, and F) and dominance (elements B and C) TRD and posterior means of the additive (elements D–F) and dominance (element D) effects, the *P*-value (elements A and B) derived from the frequentist χ^2-test, and the simulated (*i.e.*, real) additive TRD effect (element E).

2, 3, 4, and 6 (Figure 3; Figure 4; Figure 5) after correcting for multiple testing. Nevertheless, crosses 1, 4, and 6 revealed some putative, although nonsignificant, *P*-value peaks, suggesting the possibility of underlying TRD phenomena. Mouse cross 5 showed a highly significant peak on chromosome 14 ($P = 4.1\times10^{-8}$) with a relevant decrease in genotypic frequencies of both homozygotes (0.19 and 0.08). These preliminary analyses characterized a low incidence of TRD phenomena without providing very relevant information about the inheritance models underlying these departures.

The genome scans for TRD QTL under BF methodologies are also shown in Figures 3–5. Note that permutation tests revealed an upper bound for BFs (*i.e.*, posterior odds) under the hypothesis of null TRD ranging between 0.72 and 1.07. These estimates allowed for an easy interpretation of PO, where values >1 favored the TRD model even within the context of multiple testing that originated from the large number of genetic markers involved in our mouse data sets. Henceforth, these TRD QTL are referred to with the following notation: *e.g.*, $Chr3_{73}$-6_a identifies a TRD QTL on mouse chromosome 3 at 73 Mb, detected in the F_2 intercross 6 and linked to the parameter *a*. Significant dominant TRD QTL were revealed in crosses 1 ($Chr1_{111}$-1_d and $Chr3_{100}$-1_d), 4 ($Chr12_{101}$-4_d and $Chr13_{17}$-4_d), and 5 ($Chr14_{29}$-5_d) with moderate Bayes factors (∼4) except for the $Chr14_{29}$-5_d QTL in chromosome 14 (PO = 29,976.7; Table 2). Assuming Jeffreys' (1984) scale of evidence, the analyses provided decisive evidence (BF > 100) about the TRD in $Chr14_{29}$-5_d, whereas the remaining TRD QTL provide only substantial evidences (3.16 < BF < 10) and they must be taken with caution. Note that the location of the $Chr14_{29}$-5_d QTL agreed with the highly significant departure reported with the χ^2-test scanning in this F_2 cross, whereas the remaining TRD QTL agreed with the location of the putative *P*-value peaks obtained through χ^2-tests. Parameter *a* revealed three TRD QTL in chromosomes 2 ($Chr2_{144}$-6_a; PO = 1.3), 3 ($Chr3_{73}$-6_a; PO = 21.7), and 15 ($Chr15_{59}$-6_a; PO = 1.8) for mouse cross 6 (Figure 5B), although the PO in chromosomes 2 and 15 are very low according to Jeffreys (1984). On the other hand, the $Chr3_{73}$-6_a QTL falls within Jeffreys' (1984) level of strong evidence (10 < BF < 31.62), revealing this chromosomal location as a very interesting candidate region given the additive departure pattern from the expected genotypic frequencies.

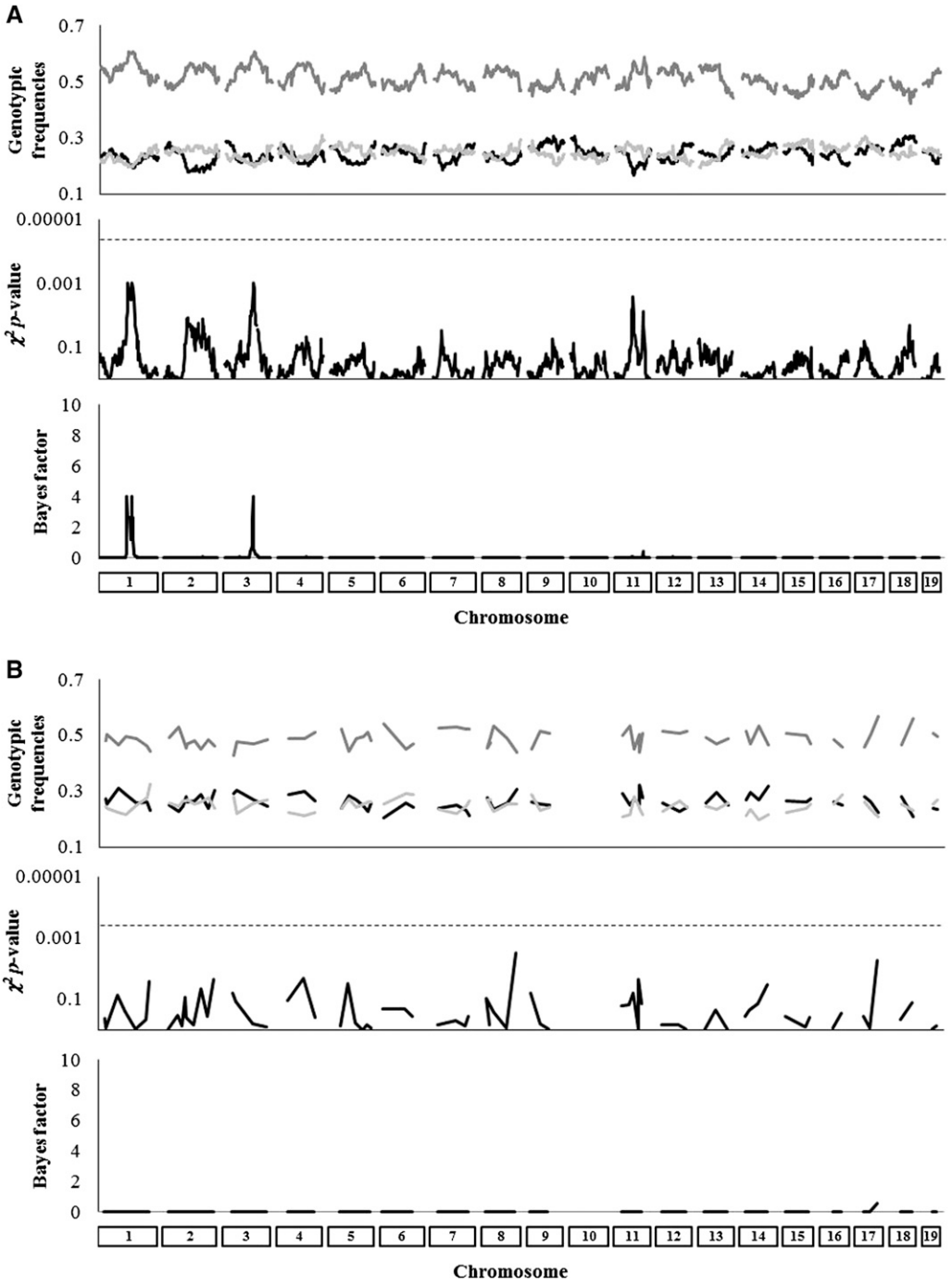

Figure 3 Diagrams of transmission ratio distortion quantitative trait loci in C57BL/6J × CAST/EiJ (cross 1) (A) and C57BL/6J$^{hg/hg}$ × CAST/EiJ (cross 2) (B) F_2 crosses with 296 and 536 mice, respectively. (Top) Observed genotypic frequencies for C57BL/6J (or C57BL/6J$^{hg/hg}$) homozygous (solid line), heterozygous (line with dark shading), and CAST/EiJ homozygous (line with light shading) populations. (Middle) *P*-value from a SNP-by-SNP χ^2-test with 2 d.f., evaluating the departure from the expected 0.25:0.5:0.25 genotypic frequencies in an F_2 population (the horizontal dotted line shows the significance threshold after a Bonferroni correction with α = 0.05). (Bottom) Plot of the posterior odds (PO) for dominance transmission ratio distortion (*i.e.*, parameter *d*). Note that the remaining TRD parameters did not provide >1 PO at any marker location in these mouse crosses.

Transmission ratio distortion effects

The location (maximum Bayes factor) and confidence intervals (*i.e.*, SNP with PO > 1) for each TRD QTL are shown in Table 2. Note that the *Chr13*$_{17}$-*4*$_d$ QTL was placed at the proximal end of the chromosome and may contain *loci* outside the region covered by SNP markers that could contribute to TRD (Figure 4B). All the TRD QTL involved several markers and the departure from the expected genotypic frequencies spanned between 1 (*Chr3*$_{73}$-*6*$_a$) and 17 Mb (*Chr1*$_{111}$-*1*$_d$), except the highly significant TRD hotspot in chromosome 14 (*Chr14*$_{29}$-*5*$_d$) that involved a unique marker (*D14mit44*). Despite its huge PO, artifacts during genotyping cannot be completely discarded for this TRD QTL. Modal estimates for the *d* parameter placed around 0.3 for *Chr1*$_{111}$-*1*$_d$, *Chr3*$_{100}$-*1*$_d$, *Chr12*$_{101}$-*4*$_d$, and *Chr13*$_{17}$-*4*$_d$, and it was 0.562 for *Chr14*$_{29}$-*5*$_d$ (Table 2). As a reference, an effect of $d = 0.3$ predicts a reduction in the genotypic frequencies of each homozygote (0.206) and, as a consequence, the heterozygous genotype is overrepresented (0.588). All three additive TRD QTL showed the same pattern, with a statistically-significant additive effect against C57BL/6$^{ob/ob}$ alleles. This additive allelic effect showed a posterior mean ranging between 0.164 (*Chr15*$_{59}$-*6*$_a$) and 0.319 (*Chr2*$_{144}$-*6*$_a$), with a posterior

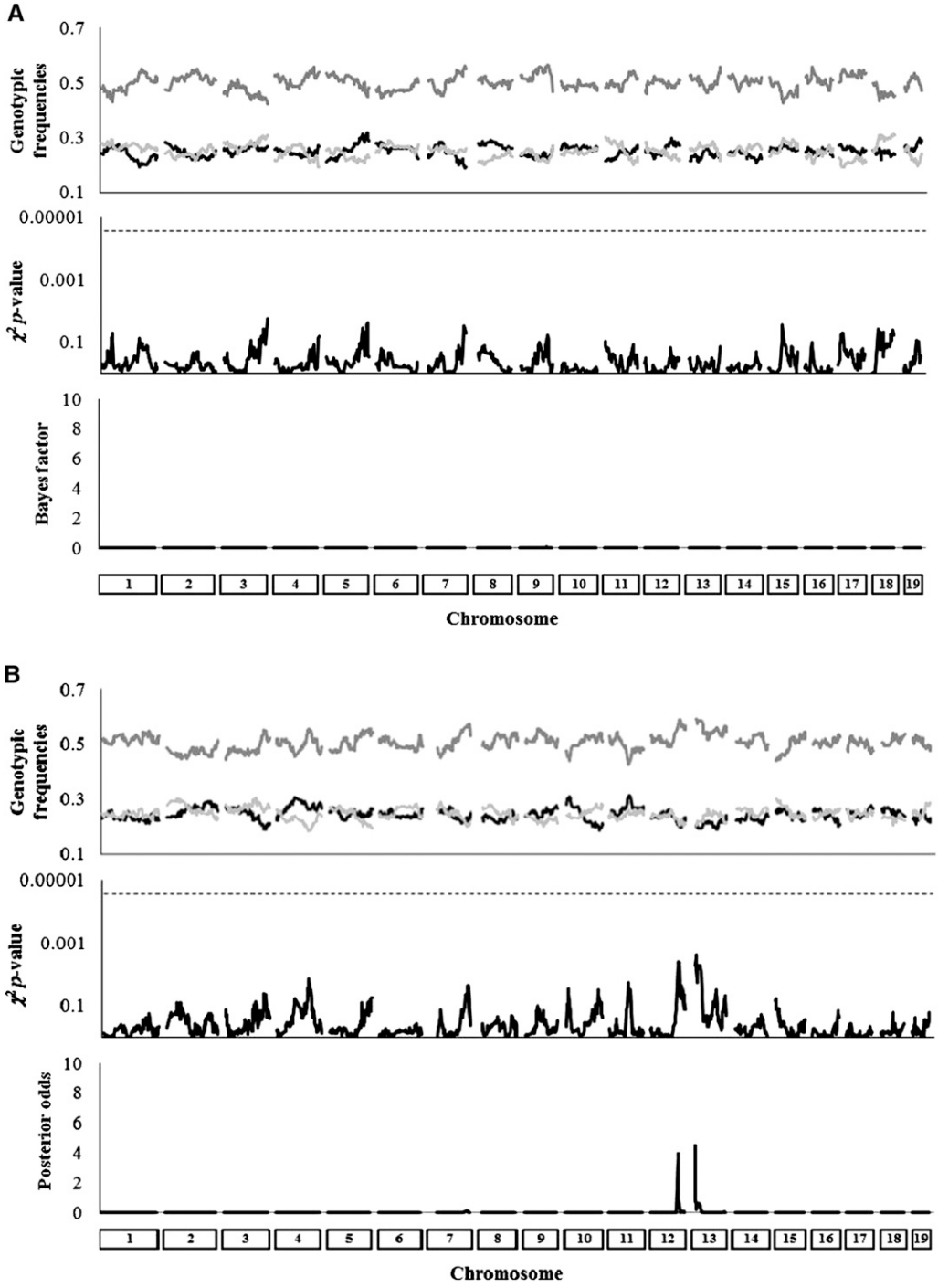

Figure 4 Diagrams of transmission ratio distortion quantitative trait loci in C57BL/6J × C3H/HeJ (cross 3) (A) and B6.apoE$^{-/-}$ × C3H.apoE$^{-/-}$ (cross 4) (B) F_2 crosses with 209 and 322 mice, respectively. (Top) Observed genotypic frequencies for C3H/HeJ (or C3H.apoE$^{-/-}$) homozygous (solid line), heterozygous (line with dark shading), and C57BL/6J (or B6.apoE$^{-/-}$) homozygous (line with light shading) populations. (Middle) *P*-value from a SNP-by-SNP χ^2-test with 2 d.f., evaluating the departure from the expected 0.25:0.5:0.25 genotypic frequencies in an F_2 population (the horizontal dotted line shows the significance threshold after a Bonferroni correction with α = 0.05). (Bottom) Plot of the posterior odds (PO) for dominance transmission ratio distortion (*i.e.*, parameter *d*). Note that the remaining TRD parameters did not provide >1 PO at any marker location in these mouse crosses.

standard deviation <0.140 in all cases (Table 2). Focusing on $Chr3_{73}$-6_a, the predicted genotypic frequencies under a pure additive pattern (*i.e.*, $d = 0$; $A/A = 0.19$; $A/B = 0.50$; $B/B = 0.31$) agreed with the observed genotypic frequencies ($A/A = 0.18$; $A/B = 0.52$; $B/B = 0.30$).

Discussion

Markers involved in segregation distortion have been suggested in several species including wildflowers (Hall and Willis 2005), crop plants (Jeczewski *et al.* 1997), trees (Yin *et al.* 2002), insects (Tan *et al.* 2001; Solignac *et al.* 2004), marine invertebrates (Li and Guo 2004), mice (de la Casa-Esperón *et al.* 2000; Lyon 2003), farm animals (Szyda *et al.* 2000), and humans (Friedrichs *et al.* 2006). Previous studies in mammals mainly focused on specific genes or chromosomal regions (Pardo-Manuel de Villena *et al.* 2000a; Lyon 2003), without characterizing the presence of TRD loci in the whole genome. The present investigation provides the first evidence of a genome-wide distribution of TRD loci in mice. TRD QTL are

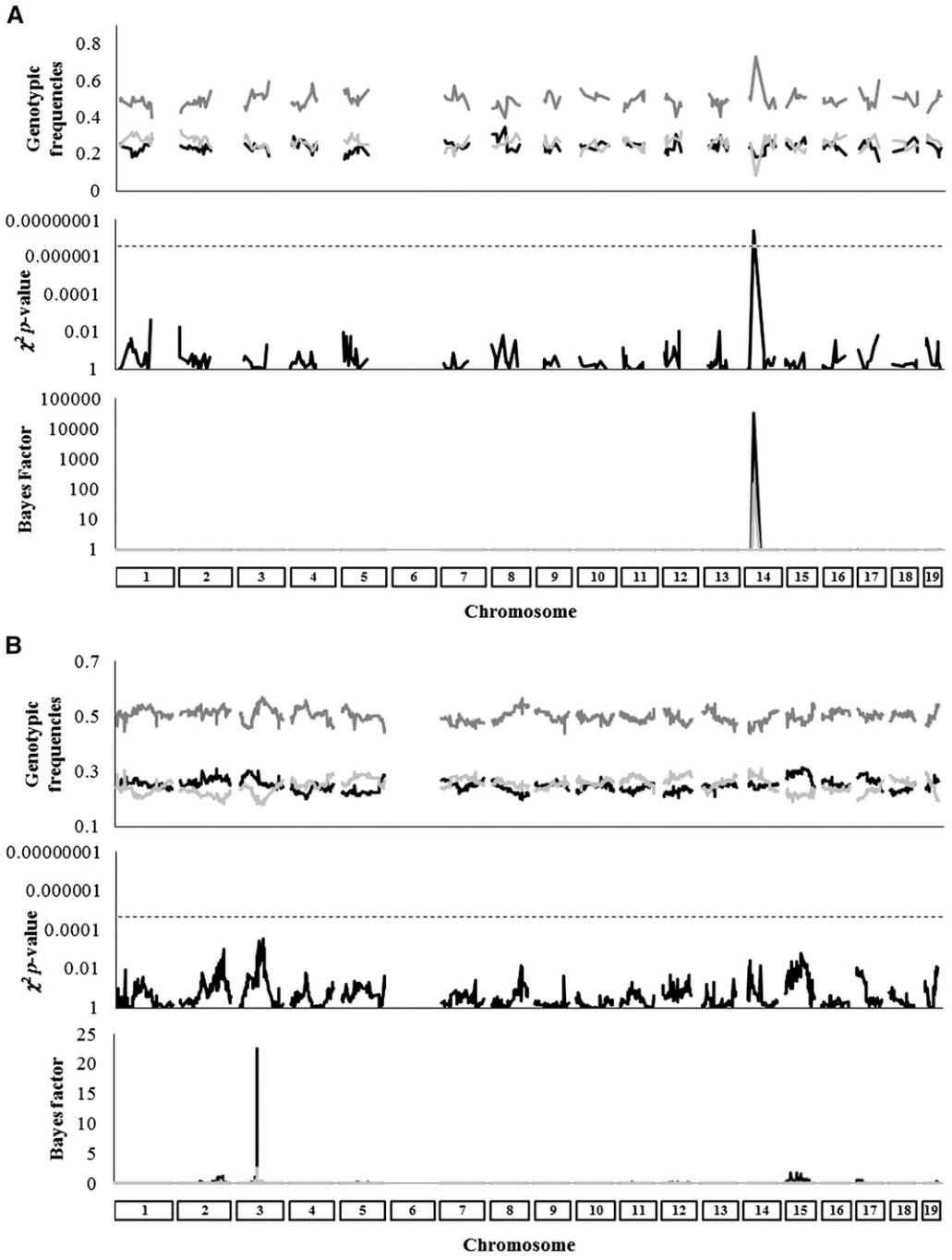

Figure 5 Diagrams of transmission ratio distortion quantitative trait loci in two C57BL/6$^{ob/ob}$ × BTBR$^{ob/ob}$ F_2 crosses with 477 (cross 5) (A) and 541 mice (cross 6) (B), respectively. (Top) Observed genotypic frequencies for BTBR$^{ob/ob}$ homozygous (solid line), heterozygous (line with dark shading), and C57BL/6$^{ob/ob}$ homozygous (line with light shading) populations. (Middle) *P*-value from a SNP-by-SNP χ^2-test with 2 d.f., evaluating the departure from the expected 0.25:0.5:0.25 genotypic frequencies in an F_2 population (the horizontal dotted line shows the significance threshold after a Bonferroni correction with $\alpha = 0.05$). (Bottom) Plots of the posterior odds (PO) for the dominance (A) and additive (B) transmission ratio distortion (*i.e.*, parameters *d* and *a*, respectively). Note that the remaining models did not provide >1 PO at any marker location in these mouse crosses.

appealing raw material for further studies of genetic mechanisms involved in segregation distortion. Also, TRD QTL provide essential information about genomic regions of complex segregation in candidate gene and QTL analyses. Note that these departures from the expected segregation percentages can bias linkage tests and the estimation of genetic distances if this TRD is not accounted for in the model (Garcia-Dorado and Gallego 1992; Lorieaux *et al.* 1995).

New models accounting for the TRD genetic mechanism

Little is known about the genetic mechanism involved in segregation departures (Shendure *et al.* 1998; de la Casa-Esperón *et al.* 2000). Even for the well-known *t* haplotype in mouse chromosome 17, the distortion pattern has been reported as variable without providing conclusive evidence of additive or dominant effects (Lyon 2003). These historical limitations were mainly due to the statistical test and the experimental design. Previous approaches focused on standard χ^2- (Montagutelli *et al.* 1996; Pardo-Manuel de Villena *et al.* 2000a; Paz-Miguel *et al.* 2001; Underfolker *et al.* 2005) and *t*-tests (Shendure *et al.* 1998), and discrepancies between genotypes were characterized in a broad sense without assessing the genetic mechanisms. TRD analyses in the mouse have been systematically performed on backcrossed

Table 2 Summary of significant transmission ratio distortion (TRD) QTL in F_2 mouse crosses

			Transmission ratio distortion QTL peak							Boundaries of the region with PO > 1	
							Genotypic freq[a]				
Cross[b]	Param[c]	Chr[d]	Marker (Mb)[e]	Posterior odds (PO)	Post mean[f]	Post SD[g]	*A/A*	*A/B*	*B/B*	Lower marker (Mb)	Upper marker (Mb)
1	*d*	1	rs3663003 (111)	4.3	0.358	0.065	0.19	0.61	0.20	rs6345367 (95)	rs3693265 (112)
1	*d*	3	rs3694780 (100)	3.9	0.330	0.076	0.20	0.60	0.20	rs3022964 (97)	rs6199015 (102)
4	*d*	12	rs3698001 (101)	4.1	0.312	0.079	0.20	0.59	0.21	rs3698001 (101)	rs4229529 (104)
4	*d*	13	rs3678616 (17)	4.5	0.331	0.068	0.20	0.60	0.20	rs3678616 (17)	rs3721858 (18)
5	*d*	14	D14Mit44 (29)	29,976.7	0.562	0.075	0.19	0.72	0.08	D14Mit44 (29)	D14Mit44 (29)
6	*a*	2	rs13476816 (144)	1.3	−0.318	0.132	0.28	0.53	0.19	rs13476801 (138)	rs13476819 (145)
6	*a*	3	rs6289734 (73)	21.7	−0.193	0.064	0.30	0.52	0.18	rs13477188 (72)	rs6289734 (73)
6	*a*	15	rs13482595 (59)	1.8	−0.163	0.127	0.32	0.47	0.21	rs13482556 (47)	rs3698351 (59)

Param, parameter; Chr, chromosome; Post mean, posterior mean; Post SD, posterior standard deviation.

[a] Genotypic frequencies characterized as *A/A* (homozygous for the allele coming from the first strain of each cross; see footnote *a*), *A/B*, and *B/B* (homozygous for the allele coming from the second strain of each cross; see footnote *b*.

[b] The F_2 crosses involved C57BL/6J × CAST/EiJ (cross 1), B6.apoE$^{-/-}$ × C3H.apoE$^{-/-}$ (cross 4), and C57BL/6$^{ob/ob}$ × BTBR$^{ob/ob}$ (crosses 5 and 6).

[c] Genetic parameter involved in the TRD phenomena (*a*, additive; *d*, dominance).

[d] Chromosome.

[e] The genomic megabase position of each marker is shown in parentheses to the right of the SNP or microsatellite identification.

[f] Posterior mean of the TRD effect.

[g] Posterior standard deviation of the TRD effect.

populations (Montagutelli *et al.* 1996; Shendure *et al.* 1998; de la Casa-Esperón *et al.* 2000), where heterozygote and only one type of homozygote animals were available. This experimental design masked the putative genetic mechanisms involved in TRD given that the departure from the expected homozygous and heterozygous frequencies could be due to additive and/or dominant effects. Hence, the Bayesian models for TRD in F_2 populations developed in this article are the first TRD-specific statistical tool allowing for the characterization of both TRD loci and their genetic mechanism. As in preceding statistical approaches, genotyping errors could impair the statistical performance of our PO, leading to improper conclusions. Although the aim of this research was not to elucidate statistical power under genotyping errors but to describe a new test for TRD, biased results can be accounted for by the use of consecutive SNP markers under linkage disequilibrium. Whereas a single-SNP–PO peak cannot be considered free from genotyping errors (Figure 5A), contiguous-SNP–PO peaks must be viewed as consistent estimates (almost) free from genotyping artifacts.

The additive or dominant (or overdominant) effects on segregation distortion were implemented as a departure term appropriately weighting each genotypic frequency and using the standard rules for allelic effects defined by Falconer and Mackay (1996). One or two genotypes were treated as a reference whereas the TRD effects were systematically subtracted from the expected genotypic frequencies of the other genotypes. The additive or dominant effects should be viewed as the departure against the reference genotype, these departures characterizing meiotic drive on gametes or fetal or neonatal failure. Overdominant effects must be related to failures after fecundation, given that the full genotype is involved during the TRD phenomenon. Both sources of TRD (gametic level or embryonic/fetal level) converge on the same "phenotypic" pattern and cannot be discriminated without additional data. This limitation could be sorted out by analyzing litter size data. A reduction in the number of pups per litter at birth would be expected if TRD was due to failure of embryos or neonates, whereas meiotic drive would not modify this parameter. Nevertheless, some male-sterility effects previously associated with TRD loci could invalidate this assumption (Pilder *et al.* 1991; Lyon 2003).

Bayes factor performance

Given that this article focuses on the development of new statistical tools, analyses on simulated data sets were performed to confirm that our BF approach was free from relevant biases. Their performance was compared with a standard χ^2-test. Note that the χ^2-test is an accepted statistical tool for TRD analyses (Nixon 2006). Results shown in Figures 1 and 2 revealed a mimicking pattern with the χ^2-test. Moreover, BFs performed well under both null and nonnull TRD phenomena, showing a direct relationship between the BF value and the estimated effect of the TRD departure. This consistency between tests suggests an appealing statistical behavior for the Bayesian analyses developed here and provides new evidence highlighting the usefulness of Verdinelli and Wasserman's (1995) BF for a particular QTL analysis. This approach was previously adapted to check several genetics-related parameters such as heritability (García-Cortés *et al.* 2001; Casellas and Piedrafita 2006), QTL (Varona *et al.* 2001, 2004; Casellas *et al.* 2008b), and inbreeding (Casellas *et al.* 2009) among others, and its performance was compared with standard frequentist approaches revealing a stable and consistent statistical behavior (Varona *et al.* 2001; Casellas *et al.* 2007, 2008a). This conclusion is supported by the similarity

between χ^2 and Bayes factor TRD QTL profiles shown in this study.

Focusing or real data, a preliminary analysis with a standard χ^2-test was performed to scan the six F_2 crosses for relevant departures from the genotypic frequencies in a broad sense. With the exception of microsatellite *D14Mit44* in cross 5, these analyses did not reveal significant departures after correcting for multiple testing, although some candidate regions were suggested by *P*-value peaks below the Bonferroni significance threshold. Both the χ^2-test and the Bayesian analyses showed similar patterns and agreed with the location of the (putative) TRD QTL (Figures 3A, 4B, and 5B).

(Over)dominance TRD QTL

Five of the eight TRD QTL ($Chr1_{111}$-1_d, $Chr3_{100}$-1_d, $Chr12_{101}$-4_d, $Chr13_{17}$-4_d, and $Chr14_{29}$-5_d) revealed a significant overexpression of the heterozygous genotype and a substantial reduction of the expected number of F_2 mice with homozygous genotypes. Although selective fertilization (Edwards 1955) depending on the genotype of both gametes cannot be completely discarded, the advantage (disadvantage) of the heterozygote (homozygote) mice suggests a genetic mechanism involved in some biological processes after fecundation, probably related to the survival failure of several homozygous individuals during the early developmental stages. This hypothesis comprises a critical period from embryo implantation until birth or even including unregistered early neonatal mortality, although the current analysis does not allow us to infer the exact physiological stage where some homozygotes died. In any case, the heterozygote overrepresentation could be directly linked to the well-known phenomenon of hybrid vigor or heterosis (Bruce 1910). This genetic mechanism involves the contribution of two unrelated breeds or strains where the performance of the F_1 progeny exceeds the expected average performance of the two founding origins (Falconer and Mackay 1996). Similarly, our results reported some chromosomal regions where the hybrid vigor theory could be extrapolated at a genomic level. These TRD QTL could suggest the presence of a *locus* with a detrimental effect on embryo or fetus viability under homozygosis, whereas these effects could be partially or completely attenuated under heterozygosis. Although this hypothesis must be corroborated in future studies, the incidence of this kind of TRD QTL in our data sets supports its relevance for F_2 populations, with important consequences for genetic analyses (Garcia-Dorado and Gallego 1992; Lorieaux *et al.* 1995).

Additive TRD QTL

The three additive TRD QTL reported for cross 6 ($Chr2_{144}$-6_a, $Chr3_{73}$-6_a, and $Chr15_{59}$-6_a) are the first evidence of TRD phenomena on mouse chromosomes 2, 3, and 15 and could be viewed as very interesting raw material for further studies to understand the genetic basis of these additive effects. Note that the additive effect could be due to influences on the gametes or on the embryo/fetus. The first option includes the preferential passage of a given allele to the oocyte or the polar bodies during meiosis (Agulnik *et al.* 1990; Wu *et al.* 2005), allele-linked effects on sperm vitality (McKee *et al.* 1998; Lyon 2003), or even selective fertilization (Edwards 1955). The second option operates at the embryo or fetus level and must imply an impaired capacity to implant to the endometrium of the uterus or embryonic or fetal lethality (Wakasugi 1974; Pardo-Manuel de Villena *et al.* 2000b), probably linked to a reduction in the average litter size.

Origin of the TRD loci

The six data sets were grouped in pairs according to the genetic background of the strains involved in each F_2 cross. Crosses 1 and 2 involved CAST and B6-related mice, crosses 3 and 4 focused on B6-related and C3H-related strains, and crosses 5 and 6 used $B6^{ob/ob}$ and $BTBR^{ob/ob}$ founder mice. Given these similarities, we could expect a reasonable correspondence between the location and the effect of the TRD QTL, at least within each pair or similar crosses. This supposition was not confirmed in our analyses (Figures 3–5). None of the TRD QTL replicated in our analyses although in some cases this may be partially due to the low density of markers available for some genome scans (crosses 2 and 5). Nevertheless, this apparent inconsistency between similar crosses suggests that our TRD QTL could be due to recent mutations, perhaps still polymorphic in the strain of origin. Recent work has revealed a continuous and relevant uploading and removal of new mutations in inbred mouse strains (Casellas and Medrano 2008; Niu and Liang 2009), and this source of genetic variation could be the origin of the TRD QTL. Thus, TRD loci or mutations must be evaluated in the specific cross where they were detected, developing an F_3 generation with a subset of F_2 mice whose recombination pattern targets a given TRD QTL, or with the use of congenic strains.

In summary, this research substantially contributes to the TRD framework with both statistical developments and the first genome-wide scans of TRD regions in mammals. The new statistical model outlined here presents a Bayesian implementation for both testing the statistical relevance of TRD patterns and characterizing the inheritance mechanism underlying these departures from the Mendelian expectation. TRD QTL were identified in several mouse chromosomes and F_2 crosses, suggesting a relevant incidence of these biological phenomena.

Acknowledgments

The authors are indebted to two anonymous referees for their helpful comments on the manuscript. This work was partially supported by National Institutes of Health grant DK69978 and by the W. K. Kellogg Endowment Fund (http://www.wkkf.org). The research contract of J. Casellas was partially financed by Spain's *Ministerio de Ciencia e Innovación* (program *Ramon y Cajal*).

Literature Cited

Agulnik, S. I., A. I. Agulnik, and A. O. Ruvinsky, 1990 Meiotic drive in female mice heterozygous for the HSR insert on chromosome 1. Genet. Res. 55: 97–100.

Bonferroni, C. E., 1930 *Elementi di Statistica Generale*. Libreria Seber, Florence, Italy.

Bruce, A. B., 1910 The Mendelian theory of heredity and the augmentation of vigor. Science 32: 627–628.

Canham, R. P., D. A. Birdsall, and D. G. Cameron, 1970 Disturbed segregation at the transferring locus of the deer mouse. Genet. Res. 16: 355–377.

Casellas, J., and J. F. Medrano, 2008 Within-generation mutation variance for litter size in inbred mice. Genetics 179: 2147–2155.

Casellas, J., and J. Piedrafita, 2006 Bayes factor for testing the genetic background of quantitative threshold traits. J. Anim. Breed. Genet. 123: 301–306.

Casellas, J., J. Piedrafita, and L. Varona, 2007 Bayes factor for testing between different structures of random genetic groups: a case study using weaning weight in Bruna dels Pirineus beef cattle. Genet. Sel. Evol. 39: 39–53.

Casellas, J., N. Ibáñez-Escriche, L. A. García-Cortés, and L. Varona, 2008a Bayes factor between Student t and Gaussian mixed models within an animal breeding context. Genet. Sel. Evol. 40: 395–413.

Casellas, J., L. Varona, G. Muñoz, O. Ramírez, A. Tomás *et al.*, 2008b Empirical Bayes factor analyses of quantitative trait loci for gestation length in Iberian × Meishan F_2 sows. Animal 2: 177–183.

Casellas, J., J. Piedrafita, G. Caja, and L. Varona, 2009 Analysis of founder-specific inbreeding depression on birth weight in Ripollesa lambs. J. Anim. Sci. 87: 72–79.

Corva, P. M., S. Horvat, and J. F. Medrano, 2001 Quantitative trait loci affecting growth in high growth (hg) mice. Mamm. Genome 12: 284–290.

Crow, J. F., 1999 Unmasking a cheating gene. Science 283: 1651.

de la Casa-Esperón, E., F. Pardo-Manuel de Villena, A. E. Verner, T. L. Briscoe, J. M. Melette *et al.*, 2000 Sex-of-offspring-specific transmission ratio distortion on mouse chromosome X. Genetics 154: 343–350.

Dyer, K. A., B. Charlesworth, and J. Jaenike, 2007 Chromosome-wide linkage disequilibrium as a consequence of meiotic drive. Proc. Natl. Acad. Sci. USA 104: 1587–1592.

Edwards, R. G., 1955 Selective fertilization following the use of sperm mixtures in the mouse. Nature 175: 215–216.

Evans, K., A. Fryer, C. Inglehearn, J. Duvall-Young, J. L. Whittaker *et al.*, 1994 Genetic linkage of cone-rod retinal dystrophy to chromosome 19q and evidence for segregation distortion. Nat. Genet. 6: 210–213.

Falconer, D. S., and T. F. C. Mackay, 1996 *Introduction to Quantitative Genetics*, Ed. 4. Longmans Green, Harlow, Essex, UK.

Friedrichs, F., S. Brescianini, V. Annese, A. Latiano, K. Berger *et al.*, 2006 Evidence of transmission ratio distortion of DLG5 R30Q variant in general and implication of an association with Crohn disease in men. Hum. Genet. 119: 305–311.

García-Cortés, L. A., C. Cabrillo, C. Moreno, and L. Varona, 2001 Hypothesis testing for the genetic background of quantitative traits. Genet. Sel. Evol. 33: 3–16.

Garcia-Dorado, A., and A. Gallego, 1992 On the use of the classical tests for detecting linkage. J. Hered. 83: 143–146.

Gelfand, A., and A. Smith, 1990 Sampling based approaches to calculating marginal densities. J. Am. Stat. Assoc. 85: 398–409.

Hall, M. C., and J. H. Willis, 2005 Transmission ratio distortion in intraspecific hybrids of *Mimulus guttatus*: implications for genetic divergence. Genetics 170: 375–386.

Hardenbol, P., F. Yu, J. Belmont, J. MacKenzie, C. Bruckner *et al.*, 2005 Highly multiplex molecular inversion probe genotyping: over 10,000 targeted SNPs genotyped in a single tube assay. Genome Res. 15: 269–275.

Hastings, W. K., 1970 Monte Carlo sampling methods using Markov chains and their application. Biometrika 57: 97–109.

Horvat, S., and J. F. Medrano, 1996 The high growth (hg) locus maps to a deletion in mouse chromosome 10. Genomics 36: 546–549.

Horvat, S., and J. F. Medrano, 2001 Lack of Socs2 expression causes the high-growth phenotype in mice. Genomics 72: 209–212.

Ingalls, A. M., M. M. Dickie, and G. D. Snell, 1950 Obese, a new mutation in the house mouse. J. Hered. 41: 317–318.

Jeffreys, H., 1984 *Theory of Probability.* Clarendon Press, Oxford, UK.

Jenczewski, E., M. Gherardi, I. Bonnon, J. M. Prosperi, I. Olivieri *et al.*, 1997 Insight on segregation distortions in two intraspecific crosses between annual species of Medicago (Leguminosae). Theor. Appl. Genet. 94: 682–691.

Kass, R. E., and A. E. Raftery, 1995 Bayes factors. J. Am. Stat. Assoc. 90: 773–795.

Li, L., and X. Guo, 2004 AFLP-based genetic linkage maps of the Pacific oyster *Crassostrea gigas* Thunberg. Mar. Biotechnol. 6: 26–36.

Lorieux, M. B., G. X. Perrier, D. Gonzalez de Leon, and C. Lanaud, 1995 Maximum likelihood models for mapping genetic markers showing segregation distortion. 1. Backcross population. Theor. Appl. Genet. 90: 73–80.

Lyon, M. F., 1991 The genetic basis of transmission-ratio distortion and male sterility due to the t-complex. Am. Nat. 137: 349–358.

Lyon, M. F., 2003 Transmission ratio distortion in mice. Annu. Rev. Genet. 37: 393–408.

McKee, B. D., K. Wilhelm, C. Merrill, and X. Ren, 1998 Male sterility and meiotic drive associated with sex chromosome rearrangements in Drosophila: role of X-Y pairing. Genetics 149: 143–155.

Merill, C., L. Bayraktaroglu, A. Kusano, and B. Ganetzky, 1999 Truncated RanGap encoded by the segregation distorter locus of Drosophila. Science 283: 1742–1745.

Merkle, S., J. Favor, J. Graw, S. Hornhardt, and W. Pretsch, 1992 Hereditary lactate dehydrogenase A-subunit deficiency as cause of early postimplantational death of homozygotes in *Mus musculus*. Genetics 131: 413–421.

Montagutelli, X., R. Turner, and J. H. Nadeau, 1996 Epistatic control of non-Mendelian inheritance in mouse specific crosses. Genetics 143: 1739–1752.

Moore, C. S., 2006 Postnatal lethality and cardiac anomalies in the Ts65Dn Down syndrome mouse model. Mamm. Genome 17: 1005–1012.

Niu, Y., and S. Liang, 2009 Genetic differentiation within the inbred C57NL/6J mouse strain. J. Zool. (Lond.) 278: 42–47.

Nixon, J., 2006 Testing for segregation distortion in genetic scoring data from backcross or doubled haploid populations. Heredity 96: 290–297.

Nur, U., 1977 Maintenance of a "parasitic" B chromosome in the grasshopper Melanouplus femur-rubrum. Genetics 87: 499–512.

Pardo-Manuel de Villena, F., E. de la Casa-Esperón, T. L. Briscoe, and C. Sapienza, 2000a A genetic test to determine the origin of maternal transmission ratio distortion: meiotic drive at the mous Om locus. Genetics 154: 333–342.

Pardo-Manuel de Villena, F., E. de la Casa-Esperón, J. W. Williams, J.-M. Malette, M. Rosa *et al.*, 2000b Heritability of the maternal meiotic drive system linked to Om and high-resolution mapping of the Responder locus in mouse. Genetics 155: 283–289.

Paz-Miguel, J., F. Pardo-Manuel de Villena, P. Sánchez-Velasco, and F. Leyva-Cobián, 2001 H2-haplotype-dependent unequal transmission of the 17^{16} translocation chromosome from Ts65Dn females. Mamm. Genome 12: 83–85.

Pilder, S. H., M. F. Hammer, and L. M. Silver, 1991 A novel mouse chromosome 17 hybrid sterility locus: implications for the origin of t haplotypes. Genetics 129: 237–246.
Raftery, A. E., and S. M. Lewis, 1992 How many iterations in the Gibbs sampler? pp. 763–773 in *Bayesian Statistics IV*, edited by J. M. Bernardo, J. O. Berger, A. P. Dawid, and A. F. M. Smith. Oxford University Press, Oxford.
Rhoades, M. M., 1942 Preferential segregation in maize. Genetics 27: 395–407.
Sargolzaei, M., F. S. Schenkel, G. B. Jansen, and L. R. Schaeffer, 2007 Extent of linkage disequilibrium in Holstein cattle in North America. J. Dairy Sci. 91: 2106–2117.
Schadt, E. E., C. Molony, E. Chudin, K. Hao, X. Yang *et al.*, 2008 Mapping the genetic architecture of gene expression in human liver. PLoS Biol. 6: e107.
Shendure, J., J. A. Melo, K. Pociask, R. Derr, and L. M. Silver, 1998 Sex-restricted non-mendelian inheritance of mouse chromosome 11 in the offspring of crosses between C57BL/6J and (C57BL/6J × DBA/2J) F_1 mice. Mamm. Genome 9: 812–815.
Shi, W., N. J. Wang, D. M. Shih, V. Z. Sun, X. Wang *et al.*, 2000 Determinants of atherosclerosis susceptibility in the C3H and C57BL/6 mouse model: evidence for involvement of endothelial cells but not blood cells on cholesterol metabolism. Circ. Res. 86: 1078–1084.
Silver, L. M., 1985 Mouse t haplotypes. Annu. Rev. Genet. 19: 179–208.
Silver, L. M., 1993 The peculiar journey of a selfish chromosome: mouse t haplotypes and meiotic drive. Trends Genet. 9: 250–254.
Solignac, M., D. Vautrin, E. Baudry, F. Mougel, A. Loiseau *et al.*, 2004 A microsatellite-based linkage map of the honeybee, *Apis Mellifera*. Genetics 167: 253–262.
Stram, D. O., and J. W. Lee, 1994 Variance component testing in longitudinal mixed effects model. Biometrics 50: 1171–1177.
Szyda, J., H. Simianer, and S. Lien, 2000 Sex ratio distortion in bovine sperm correlates to recombination in the pseudoautosomal region. Genet. Res. 75: 53–59.
Tan, Y.- D., C. Wan, and Y. Zhu, C. Lu, Z. Xiang *et al.*, 2001 An amplified fragment length polymorphism map of the silk-worm. Genetics 157: 1277–1284.
Underkoffler, L. A., L. E. Mitchell, Z. S. Abdulali, J. N. Collins, and R. J. Oakey, 2005 Transmission ratio distortion in offspring of mouse heterozygous carriers of a (7.18) Robertsonian translocation. Genetics 169: 843–848.
Varona, L., L. A. García-Cortés, and M. Pérez-Enciso, 2001 Bayes factors for detection of quantitative trait loci. Genet. Sel. Evol. 33: 133–152.
Varona, L., L. Gómez-Raya, W. M. Rauw, A. Clop, C. Ovilo *et al.*, 2004 Derivation of a Bayes factor to distinguish between linked or pleiotropic quantitative trait loci. Genetics 166: 1025–1035.
Verdinelli, I., and L. Wasserman, 1995 Computing Bayes factors using a generalization of the Savage-Dickey density ratio. J. Am. Stat. Assoc. 90: 614–618.
Vidal, O., J. L. Noguera, M. Amills, L. Varona, M. Gil *et al.*, 2005 Identification of carcass and meat quality quantitative trait loci in a Landrace pig population selected for growth and leanness. J. Anim. Sci. 83: 293–300.
Vogl, C., and S. Xu, 2000 Multipoint mapping of viability and segregation distorting loci using molecular markers. Genetics 155: 1439–1447.
Vongs, A., T. Kakutani, R. A. Martienssen, and E. J. Richards, 1993 Arabidopsis thaliana DNA methylation mutants. Science 260: 1926–1928.
Vorechovsky, I., A. D. Webster, A. Plebani, and L. Hammarstrom, 1999 Genetic linkage of IgA deficiency to the major histocompatibility complex: evidence for allele segregation distortion, parent-of-origin penetrance differences, and the role of anti-IgA antibodies in disease predisposition. Am. J. Hum. Genet. 64: 1096–1109.
Wakasugi, N., 1974 A genetically determined incompatibility system between spermatozoa and eggs leading to embryonic death in mice. J. Reprod. Fertil. 41: 85–96.
Wang, C. S., J. J. Rutledge, and D. Gianola, 1994 Bayesian analysis of mixed linear models via Gibbs sampling with an application to litter size in Iberian pigs. Genet. Sel. Evol. 26: 91–115.
Wong, M. L., A. Islas-Trejo, and J. F. Medrano, 2002 Structural characterization of the mouse high growth deletion and discovery of a novel fusion transcript between suppressor of cytokine signaling-2 (Socs-2) and viral encoded semaphoring receptor (Plexin C1). Gene 299: 153–163.
Wu, G., L. Hao, Z. Han, S. Gao, K. E. Latham *et al.*, 2005 Maternal transmission ratio distortion at the mouse Om locus results from meiotic drive at the second meiotic division. Genetics 170: 327–334.
Yin, T., Z. Zhang, M. Huang, M. Wang, Q. Zhuge *et al.*, 2002 Molecular linkage maps of the *Populus* genome. Genome 45: 541–555.
Zhang, Y., R. Proneca, M. Maffei, M. Barone, L. Loepold *et al.*, 1994 Positional cloning of mouse obese gene and its human homologue. Nature 372: 425–432.

Communicating editor: F. F. Pardo Manuel de Villena